

# First-principles Calculation of Transition-metal $L_{2,3}$ -edge Electron-energy-loss Near-edge structures Based on Direct Diagonalization of the Many-electron Hamiltonian

Kazuyoshi Ogasawara\*, Toru Miyamae, Isao Tanaka and Hirohiko Adachi

Department of Materials Science and Engineering, Kyoto University, Kyoto 606-8501, Japan

First-principles relativistic configuration-interaction (CI) calculations of cation  $L_{2,3}$ -edge electron-energy-loss near-edge structures (ELNES) of SrTiO<sub>3</sub>, NiO and CaF<sub>2</sub> have been carried out based on the direct approach where the ground state (GS) configuration and the excited state (ES) configuration were calculated simultaneously by direct diagonalization of the many-electron Hamiltonian. The obtained theoretical spectra were compared with our recent results based on the indirect approach where the GS configuration and the ES configuration were calculated separately and their energy separation was adjusted to the value predicted by the Slater's transition-state calculation. Although both approaches well reproduced the overall features of the experimental spectra, the direct approach tend to slightly overestimate the absolute transition energies. In the case of Ti  $L_{2,3}$ -edge of SrTiO<sub>3</sub>, however, the absolute transition energies calculated by the direct approach were comparable to those by the indirect approach and were also in good agreement with experimental values, indicating sufficient inclusion of electron correlations through pure configuration interactions.

(Received March 4, 2002; Accepted April 15, 2002)

**Keywords:** electron-energy-loss near-edge structures (ELNES), first-principles calculation, relativistic effects, many-electron effects

## 1. Introduction

In recent years, electron-energy-loss near-edge structures (ELNES) have attracted increasing attention as an effective tool for materials characterization because of their sensitivity to the local electronic structures around probe atoms. For unambiguous interpretation of experimental ELNES, a reliable non-empirical computational method is indispensable. Thanks to the recent development of variety of electronic structure calculation programs, many researchers are actively reporting first-principles calculations of ELNES for variety of materials.<sup>1,2)</sup> However, in the case of 3d transition-metal (TM)  $L_{2,3}$ -edge ELNES, there are still significant computational difficulties which hinder the application of ordinary non-relativistic calculation based on the one-electron approximation.

The 3d TM  $L_{2,3}$ -edges mainly correspond to electric-dipole transitions from TM core 2p levels to unoccupied TM 3d levels. Therefore the spin-orbit splitting of core 2p levels requires the inclusion of relativistic effects while the interaction between core hole and localized d electrons requires the consideration of many-body effects.

In order to take both effects into account, we have recently developed a first-principles relativistic configuration-interaction computation code and reported the first-principles calculations of cation  $L_{2,3}$ -edge ELNES of SrTiO<sub>3</sub>, NiO and CaF<sub>2</sub> for the first time.<sup>3)</sup> In that work, we have adopted an approach where the ground state (GS) configuration and the excited state (ES) configuration were calculated separately and their energy separation was adjusted to the value predicted by the Slater's transition-state calculation (hereafter referred to as "indirect approach").

However, in principle, the GS configuration and the ES configuration should be calculated simultaneously by direct

diagonalization of the many-electron Hamiltonian (hereafter referred to as "direct approach"). Although the direct approach can significantly simplify both computational procedure and analytical process, investigation of its accuracy is also indispensable prior to using it for analysis of experimental ELNES. Therefore, in the present work, we have carried out first-principles calculation of cation  $L_{2,3}$ -edge ELNES of SrTiO<sub>3</sub>, NiO and CaF<sub>2</sub> by the direct approach and investigated the accuracy of the obtained theoretical spectra in comparison with our previous ones by the indirect approach.

## 2. Computational Procedure

### 2.1 Model clusters

For the calculation of theoretical cation  $L_{2,3}$ -edge ELNES, model clusters composed of the excited cation and the nearest neighbor anions, that is, (TiO<sub>6</sub>)<sup>8-</sup> for the Ti  $L_{2,3}$ -edge of SrTiO<sub>3</sub>, (NiO<sub>6</sub>)<sup>10-</sup> for the Ni  $L_{2,3}$ -edge of NiO, and (CaF<sub>8</sub>)<sup>6-</sup> for the Ca  $L_{2,3}$ -edge of CaF<sub>2</sub>, were constructed based on the crystal structure of each compound. All these clusters possess octahedral ( $O_h$ ) symmetry. The effective Madelung potential was taken into account by locating several thousand point charges at the external atomic positions.

### 2.2 Relativistic MO calculation

The relativistic molecular orbital (MO) calculations were performed self-consistently based on the Dirac-Fock-Slater method using the relativistic SCAT computation code, originally developed by Rosén *et al.*<sup>4)</sup> In this code, molecular orbitals were calculated as linear combination of atomic orbitals (LCAO). The four component relativistic atomic orbitals were produced in each iteration and optimized to the chemical environment. The basis functions adopted in the present work were 1s~4p for Ti, Ni, Ca and 1s~2p for O, F. All integrals were performed numerically using 100000 pseudorandom sampling points.

\*Present address: School of Science and Technology, Kwansei Gakuin University, 2-1 Gakuen, Sanda 669-1377, Japan.

### 2.3 Direct approach

Since the CI calculation for all  $N$  electrons is unrealistically demanding, we adopted a relativistic many-electron Hamiltonian for selected  $n$  electrons, which can be expressed as,

$$H = \sum_{i=1}^n h(\mathbf{r}_i) + \sum_{i=1}^n \sum_{j>i}^n \frac{1}{|\mathbf{r}_i - \mathbf{r}_j|}, \quad (2.1)$$

where

$$h(\mathbf{r}_i) = c\boldsymbol{\alpha}\mathbf{p}_i + \beta c^2 - \sum_{\nu} \frac{Z_{\nu}}{|\mathbf{r}_i - \mathbf{R}_{\nu}|} + V_0(\mathbf{r}_i), \quad (2.2)$$

in atomic units ( $m = e = \hbar = 1$ ). Here  $\boldsymbol{\alpha}$ ,  $\beta$  are the Dirac matrices,  $c$  is the velocity of light,  $\mathbf{p}_i$  is the momentum operator,  $Z_{\nu}$  is the charge of the  $\nu$ th nucleus, and  $V_0(\mathbf{r})$  is the potential from the other  $N - n$  electrons. The explicit form of  $V_0(\mathbf{r})$  was derived by Watanabe and Kamimura.<sup>5)</sup>

In the direct approach, the above Hamiltonian was diagonalized using all Slater determinants corresponding to the GS or ES configuration. The many-electron wave functions were then generally expressed as a linear combination of the Slater determinants,

$$\Psi_i = \sum_{p=1}^M C_{ip} \Phi_p, \quad (2.3)$$

where  $M$  is the total number of the Slater determinants.

### 2.4 Indirect approach

In the indirect approach, the GS configuration and the ES configuration were diagonalized separately and the energy separation between these configurations was adjusted to the value calculated by the Slater's transition state method, where the total energy difference between two configurations can be approximately obtained by the one-electron energy difference calculated in the Slater's transition state.<sup>6)</sup> The transition energy in many-electron picture and that in one-electron picture are schematically shown in Fig. 1. In the present work, transitions with lowest transition-energies in the one-electron picture were used as the reference to determine the energy separation between the GS configuration and the ES configuration.

### 2.5 Oscillator strength

The oscillator strength of the electric-dipole transition averaged over all polarizations is generally expressed as,

$$I_{if} = \frac{2}{3} (E_f - E_i) |\langle \Psi_i | \sum_{j=1}^n \mathbf{r}_j | \Psi_f \rangle|^2 \quad (2.4)$$

where  $\Psi_i$  and  $\Psi_f$  are the many-electron wave functions for the initial state and the final state, while  $E_i$  and  $E_f$  are their energies.

### 2.6 Electronic configurations

The relativistic CI calculations were carried out within the subspace spanned by Slater determinants corresponding to the GS configuration and ES configuration with one excited electron. In the case of  $\text{Ti}^{4+}$  and  $\text{Ca}^{2+}$ , for example, the GS configuration is  $(2p)^6(\phi_{3d})^0$  and the ES configuration is

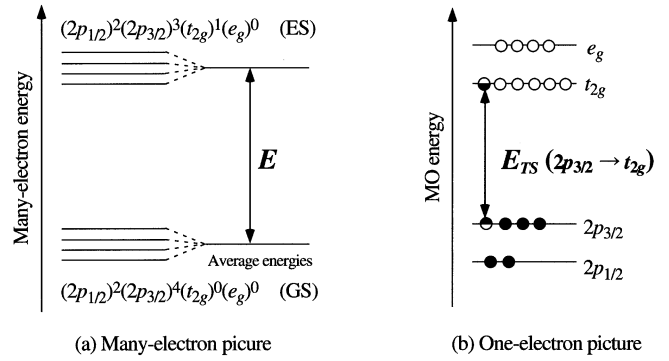


Fig. 1 Schematic illustrations of (a) transition energy in the many-electron picture and (b) that in the one-electron picture (Slater's transition-state method). In the direct approach, the ground-state (GS) configuration and the excited-state (ES) configuration are diagonalized simultaneously and their energy separation is determined automatically. On the other hand, in the indirect approach, the GS configuration and the ES configuration are diagonalized separately and their energy separation,  $E$ , is set at the value obtained by the Slater's transition state method,  $E_{TS}$ .

$(2p)^5(\phi_{3d})^1$ , where  $\phi_{3d}$  represents the MOs mainly composed of  $3d$  orbitals. Therefore, six electrons and sixteen orbitals were treated explicitly. In the indirect approach, the numbers of Slater determinants used in the diagonalization of the many-electron Hamiltonian are 1 and 60 ( $= {}_6C_1 \times {}_{10}C_1$ ) for GS and ES configurations, respectively. In the direct approach, the many-electron Hamiltonian was diagonalized using all these 61 Slater determinants.

In the case of  $\text{Ni}^{2+}$ , the GS configuration is  $(2p)^6(\phi_{3d})^8$  and the ES configuration is  $(2p)^5(\phi_{3d})^9$ . Therefore, fourteen electrons and sixteen orbitals were treated explicitly. In the indirect approach, the numbers of Slater determinants used in the diagonalization of the many-electron Hamiltonian are 45 ( ${}_{10}C_8$ ) and 60 ( $= {}_6C_1 \times {}_{10}C_9$ ) for GS and ES configurations, respectively. In the direct approach, the many-electron Hamiltonian was diagonalized using all these 105 Slater determinants.

## 3. Results and Discussions

### 3.1 SrTiO<sub>3</sub>

The theoretical Ti  $L_{2,3}$ -edge ELNES spectra of SrTiO<sub>3</sub> calculated by the direct approach and the indirect approach are compared with the experimental spectrum reported by Van der Laan<sup>7)</sup> in Fig. 2(a), where each peak in the theoretical spectra was broadened by a Gaussian function with 1.0-eV full width at half maximum (FWHM) for easy comparison. In the indirect approach,  $2p_{3/2} \rightarrow t_{2g}$  transition was used as the reference. Therefore, the Slater's transition state calculation was carried out in the  $(2p_{1/2})^2(2p_{3/2})^{7/2}(t_{2g})^{1/2}(e_g)^0$  configuration and the transition energy was calculated as  $E_{TS} = \varepsilon_{t_{2g}} - \varepsilon_{2p_{3/2}} = 457.3$  eV, where  $\phi_{3d}$  with  $t_{2g}$  and  $e_g$  symmetry are represented by the corresponding irreducible representations for simplicity and one-electron energies are represented by  $\varepsilon$ . Since this transition corresponds to the transition from  $(2p_{1/2})^2(2p_{3/2})^4(t_{2g})^0(e_g)^0$ , to  $(2p_{1/2})^2(2p_{3/2})^3(t_{2g})^1(e_g)^0$  in the many-electron picture, the difference between the average energies of these configurations was set at 457.3 eV in the indirect approach.

The experimental spectrum shows relatively large peaks  $c$ ,

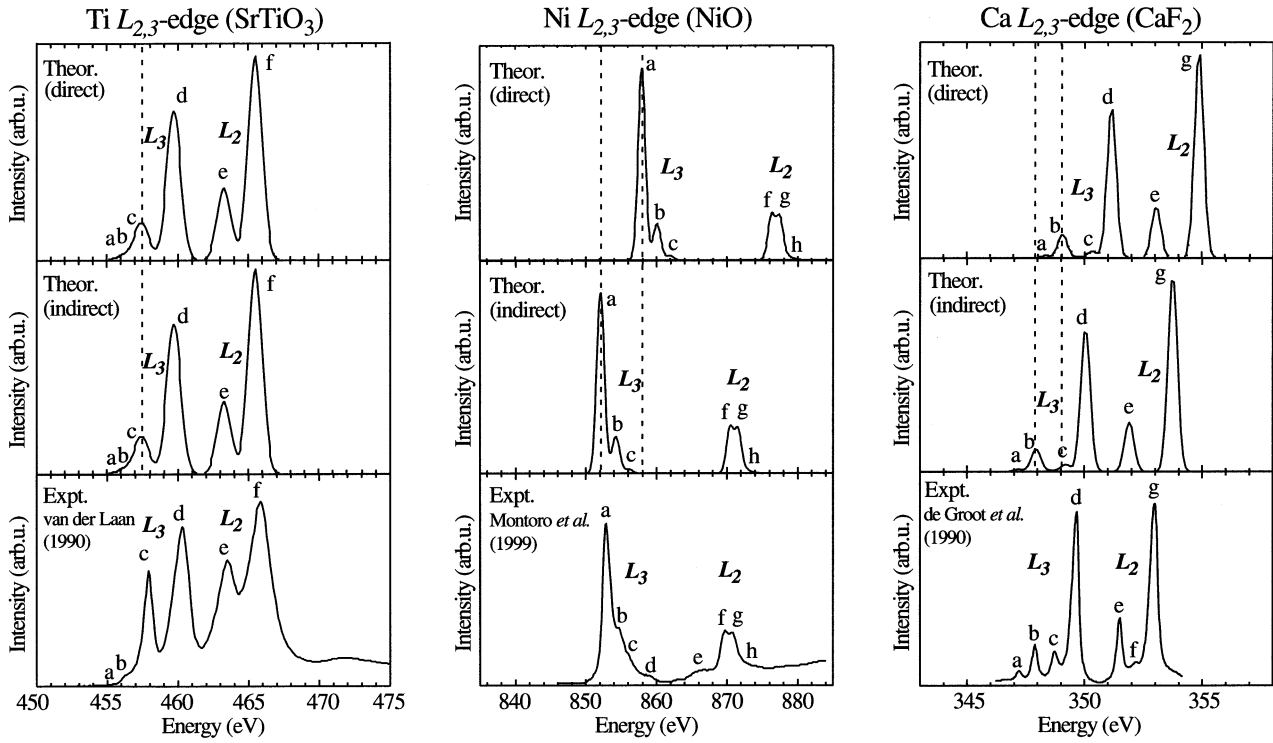


Fig. 2 Theoretical and experimental  $L_{2,3}$ -edge ELNES spectra for (a)  $\text{Ti}^{4+}$  in  $\text{SrTiO}_3$ , (b)  $\text{Ni}^{2+}$  in  $\text{NiO}$ , and (c)  $\text{Ca}^{2+}$  in  $\text{CaF}_2$ . The top and middle panels represent the theoretical spectra calculated by the direct approach and the indirect approach, respectively. The bottom panels represent the experimental spectra reported by several authors.<sup>7,8,10</sup> The positions of the most prominent peaks in the threshold configurations are indicated by dotted lines in the theoretical spectra.

$d$ ,  $e$ , and  $f$ , and small peaks  $a$  and  $b$ . As shown in the figure, both theoretical approaches reproduced the positions and relative intensities of all these peaks. According to the configuration analysis of the many-electron wave functions, peaks  $a$ ,  $b$ , and  $c$  are mainly ascribed to  $2p_{3/2} \rightarrow t_{2g}$  transition while peaks  $d$ ,  $e$ , and  $f$  are mainly ascribed to  $2p_{3/2} \rightarrow e_g$ ,  $2p_{1/2} \rightarrow t_{2g}$ , and  $2p_{1/2} \rightarrow e_g$  transitions, respectively. Since the configuration analysis indicated that peak  $c$  is the most prominent peak corresponding to the above reference transition, we evaluated the absolute transition energy by the position of this peak. The theoretically predicted position of peak  $c$  is 457.4 eV and 458.2 eV for the direct approach and for the indirect approach, respectively. Both of them are in excellent agreement with the experimental value, 457.9 eV.

### 3.2 NiO

The theoretical Ni  $L_{2,3}$ -edge ELNES spectra of NiO calculated by the direct approach and the indirect approach are compared with the experimental spectrum reported by Montoro *et al.*<sup>8</sup>) in Fig. 2(b), where each peak in the theoretical spectra was broadened by a Gaussian function with 1.0 eV FWHM for easy comparison. In the indirect approach, the  $2p_{3/2}$  to  $e_g$  transition was used as the reference. Therefore, the Slater's transition state calculation was carried out in the  $(2p_{1/2})^2(2p_{3/2})^7(t_{2g})^6(e_g)^{5/2}$  configuration and the transition energy was calculated as  $E_{TS} = \varepsilon_{e_g} - \varepsilon_{2p_{3/2}} = 851.3$  eV. Since this transition corresponds to the transition from  $(2p_{1/2})^2(2p_{3/2})^4(t_{2g})^6(e_g)^2$ , to  $(2p_{1/2})^2(2p_{3/2})^3(t_{2g})^6(e_g)^3$  in the many-electron picture, the difference between the average energies of these configurations was set at 851.3 eV in the indirect approach.

The experimental Ni  $L_{2,3}$ -edge ELNES of NiO shows relatively large peaks  $a$ ,  $b$ ,  $f$  and  $g$  and small peaks  $c$ ,  $d$ ,  $e$ , and  $h$ . As shown in the figure, both theoretical approaches reproduced the relative positions and relative intensities of these peaks except  $d$  and  $e$  which are related to the creation of the ligand hole.<sup>9</sup>) According to the configuration analysis of the many-electron wave functions peaks  $a$ ,  $b$  are mainly ascribed to  $2p_{3/2} \rightarrow e_g$  transition and peaks  $f$  and  $g$  are mainly ascribed to  $2p_{1/2} \rightarrow e_g$  transition. On the other hand, the small peak  $c$  mainly corresponds to a two electron excitation ( $2p_{3/2} \rightarrow e_g$  and  $t_{2g} \rightarrow e_g$ ), while the small peak  $h$  also corresponds to a similar two electron excitation ( $2p_{1/2} \rightarrow e_g$  and  $t_{2g} \rightarrow e_g$ ). These two-electron excitations are slightly allowed through the small composition of one-electron excitation states mixing through configuration interactions. Since the configuration analysis indicated that peak  $a$  is the most prominent peak corresponding to the above reference transition, we evaluated the absolute transition energy by the position of this peak. The theoretically predicted position of peak  $a$  is 857.9 eV and 852.1 eV for the direct approach and for the indirect approach, respectively. Therefore, the value by the indirect approach is in good agreement with the experimental value 852.8 eV, however, the theoretical value by the direct approach is slightly overestimated.

### 3.3 CaF<sub>2</sub>

The theoretical Ca  $L_{2,3}$ -edge ELNES spectra of  $\text{CaF}_2$  calculated by the direct approach and the indirect approach are compared with the experimental spectrum reported by de Groot *et al.*<sup>10</sup>) in Fig. 2(c), where each peak in the theoretical spectra was broadened by a Gaussian function

with 0.4-eV FWHM for easy comparison. In the indirect approach, the  $2p_{3/2}$  to  $e_g$  transition was used as the reference. Therefore, the Slater's transition state calculation was carried out in the  $(2p_{1/2})^2(2p_{3/2})^{7/2}(e_g)^{1/2}(t_{2g})^0$  configuration and the transition energy was calculated as  $E_{TS} = \varepsilon_{e_g} - \varepsilon_{2p_{3/2}} = 347.7$  eV. Since this transition corresponds to the transition from  $(2p_{1/2})^2(2p_{3/2})^4(e_g)^0(t_{2g})^0$ , to  $(2p_{1/2})^2(2p_{3/2})^3(e_g)^1(t_{2g})^0$  in the many-electron picture, the difference between the average energies of these configurations was set at 347.7 eV in the indirect approach.

The experimental spectrum shows relatively large peaks  $b$ ,  $d$ ,  $e$ , and  $g$ , and small peaks  $a$  and  $c$ . As shown in the figure, both theoretical approaches reproduced the positions and relative intensities of all these peaks. According to the configuration analysis of the many-electron wave functions, peaks  $a$  and  $b$  are mainly ascribed to  $2p_{3/2} \rightarrow e_g$  transition and peaks  $c$  and  $d$  are mainly ascribed to  $2p_{3/2} \rightarrow t_{2g}$  transition, while peaks  $e$  and  $g$  are mainly ascribed to  $2p_{1/2} \rightarrow e_g$ , and  $2p_{1/2} \rightarrow t_{2g}$  transitions, respectively. Since the configuration analysis indicated that peak  $b$  is the most prominent peak corresponding the above reference transition, we decided to evaluate the absolute transition energy by the position of peak  $b$ . The theoretically predicted position of peak  $b$  is 349.1 eV and 347.9 eV for the direct approach and for the indirect approach, respectively. Therefore, the value by the indirect approach is in good agreement with the experimental value 347.9 eV, however, the theoretical value by the direct approach is slightly overestimated.

### 3.4 Effect of electron correlations

In the indirect approach, energy separation between the ES configuration and the GS configuration is determined by the Slater's transition state calculation, where electron correlation effects are included in the form of orbital relaxations. Therefore the indirect approach can partially include correlation effects of all electrons. The accuracy of the results of the indirect approach indicates that such effects are taken into account sufficiently.

On the other hand, in the direct approach, electron correlations are taken into account only through configuration interactions. In the present work, some electrons are explicitly treated, while others are completely frozen. According to the results of the direct approach, theoretical transition energies tend to be slightly overestimated except Ti  $L_{2,3}$ -edge. Therefore, the accuracy of this approach is sensitive to the systems to be calculated. The accuracy of the calculated transition energy of Ti  $L_{2,3}$ -edge indicated that electron correlations can be taken into account sufficiently only through configuration

interactions for this system.

## 4. Conclusion

In the present work, we have carried out first-principles relativistic configuration-interaction (CI) calculation of cation  $L_{2,3}$ -edge ELNES by direct diagonalization of the many-electron Hamiltonian (direct approach) and compared the obtained theoretical spectra with our previous results calculated by the indirect approach. The results can be summarized as follows. (1) The overall features of the experimental spectra were well reproduced both in the direct approach and the indirect approach. (2) The direct approach tend to slightly overestimate the absolute transition energies. (3) In the case of Ti  $L_{2,3}$ -edge of SrTiO<sub>3</sub>, the direct approach well reproduced absolute transition energies.

These results indicate that we can use the direct approach for the analysis of already obtained experimental ELNES. However, since the accuracy of the absolute transition energies calculated by the direct method are rather sensitive to the materials, the indirect approach is still preferable for quantitative prediction of completely unknown spectra. The clarification of the detailed condition under which the direct approach can provide sufficiently accurate results would be important for the future establishment of efficient and reliable approach for analysis of variety of ELNES spectra.

## Acknowledgements

This work was supported by a Grant-in-Aid for Scientific Research from the Ministry of Education, Science, Sports and Culture.

## REFERENCES

- 1) S. Köstlemer and C. Elsässer: Phys. Rev. **B60** (1999) 14025.
- 2) S.-D. Mo and W. Y. Ching: Phys. Rev. **B62** (2000) 7901.
- 3) K. Ogasawara, T. Iwata, Y. Koyama, T. Ishii, I. Tanaka and H. Adachi: Phys. Rev. **B64** (2001) 115413.
- 4) A. Rosén, D. E. Ellis, H. Adachi and F. W. Averill: J. Chem. Phys. **65** (1976) 3629.
- 5) S. Watanabe and H. Kamimura: Mater. Sci. Eng. **B3** (1989) 313.
- 6) J. C. Slater: *Quantum Theory of Molecules and Solids*, Vol. 4 (McGraw-Hill, New York, 1974).
- 7) G. van der Laan: Phys. Rev. **B41** (1990) 12366.
- 8) L. A. Montoro, M. Abbate, E. C. Almeida and J. M. Rosolen: Chem. Phys. Lett. **309** (1999) 14.
- 9) G. van der Laan, J. Zaanen, G. A. Sawatzky, R. Karnatak and J.-M. Esteva: Phys. Rev. **B33** (1986) 4253.
- 10) F. M. F. de Groot, J. C. Fuggle, B. T. Thole and G. A. Sawatzky: Phys. Rev. **B41** (1990) 928.